

## Experimental evidence of locally resonant sonic band gap in two-dimensional phononic stubbed plates

Mourad Oudich,<sup>1</sup> Matteo Senesi,<sup>2</sup> M. Badreddine Assouar,<sup>1,3,\*</sup> Massimo Ruzenne,<sup>2</sup> Jia-Hong Sun,<sup>4</sup> Brice Vincent,<sup>1</sup> Zhilin Hou,<sup>5</sup> and Tsung-Tsong Wu<sup>4</sup>

<sup>1</sup>*Institut Jean Lamour, Department of Physics, CNRS, Nancy University, Nancy, France*

<sup>2</sup>*Daniel Guggenheim School of Aerospace Engineering, Georgia Institute of Technology, Atlanta, Georgia, USA*

<sup>3</sup>*International Joint Laboratory (UMI 2958), CNRS-GIT, Georgia Institute of Technology, Atlanta, Georgia, USA*

<sup>4</sup>*Institute of Applied Mechanics, National Taiwan University, Taipei 106, Taiwan*

<sup>5</sup>*Department of Physics, South China University of Technology, Guangzhou, China*

(Received 29 July 2011; revised manuscript received 10 October 2011; published 31 October 2011)

We provide experimental evidence of the existence of a locally resonant sonic band gap in a two-dimensional stubbed plate. Structures consisting of a periodic arrangement of silicone rubber stubs deposited on a thin aluminium plate were fabricated and characterized. Brillouin spectroscopy analysis is carried out to determine the elastic constants of the used rubber. The constants are then implemented in an efficient finite-element model that predicts the band structure and transmission to identify the theoretical band gap. We measure a complete sonic band gap for the out-of-plane Lamb wave modes propagating in various samples fabricated with different stub heights. Frequency domain measurements of full wave field and transmission are performed through a scanning laser Doppler vibrometer. A complete band gap from 1.9 to 2.6 kHz is showed using a sample with 6-mm stub diameter, 5-mm thickness, and 1-cm structure periodicity. Very good agreement between numerical and experimental results is obtained.

DOI: [10.1103/PhysRevB.84.165136](https://doi.org/10.1103/PhysRevB.84.165136)

PACS number(s): 43.20.+g, 43.35.+d, 46.40.Cd, 63.20.Pw

### I. INTRODUCTION

The propagation of elastic waves in periodic structures composed of multiple components has received much attention over the past decade because of their unique physical properties and large number of potential applications.<sup>1–5</sup> These composite materials, called phononic crystals (PCs), are of special interest because they may give rise to complete band gaps (BGs) that can prohibit elastic wave propagation in any direction. The existence of complete frequency BGs may lead to developing phononic circuits, perfect acoustic mirrors, and sound isolation.<sup>6–10</sup> The band gaps may originate from Bragg scattering, resulting from the periodicity of the structure, or may due to the existence of local resonances (LRs) in each unit cell. For the first mechanism, the BG usually falls into the wavelength region of the order of the structural period, but for the second one, a resonant BG is imposed by the frequency of resonance associated with scattering units and depends less on the periodicity and the symmetry of the structure. Generally, the BG frequency range based on this mechanism can be almost two orders of magnitude lower than the usual Bragg gap in the frequency region. In most of the previous works<sup>4,5,11–14</sup> about locally resonant phononic crystals (LRPCs), the proposed structures are made of LR units with soft materials, or a heavy core coated with soft materials, embedded in a hard matrix, forming a two-dimensional (2D) or three-dimensional (3D) infinite system. In those structures, low-frequency BGs for bulk waves can be obtained. Recently, a 2D LR thin-plate structure was studied theoretically by Hsu *et al.*<sup>11</sup> and Xiao *et al.*,<sup>15</sup> and they suggested that a LR BG of Lamb wave modes can also be obtained by filling soft rubber in holes drilled periodically in a thin elastic plate.

From a practical point of view, many applications in acoustics, such as traffic noise shielding or building insulation, require a gap at low frequencies. For instance, for aircraft

acoustical linings, the low-frequency audible range<sup>13</sup> (about 800 Hz to 10 kHz) is of great importance for the human quality of life. The band gap structure is not suitable to be large-scale and heavy. Therefore, a band gap structure for a sonic regime without enlarging the lattice constant can be conceived based on a LR mechanism.

In this paper, a 2D locally resonant phononic crystal composed of a periodic arrangement of silicone rubber stubs deposited on a thin aluminum homogenous plate is experimentally investigated. We show that the proposed structure can be prepared easily and that the physical behavior behind it can be presented clearly. Experimental evidence of a locally resonant sonic band gap of the studied stubbed phononic plates is shown and discussed.

The paper is organized as follow. In Sec. II, we present the numerical and physical models, the geometry and the fabrication of the structure. Then, we present the characterization methods we used to measure the physical properties of the materials composing the phononic structure and the band gap, that is, Brillouin spectroscopy (BS) and scanning laser Doppler vibrometry (SLDV). In Sec. III 1, we determine experimentally the elastic constants of silicone rubber used in our structures. Second (Sec. III.2), we compute the band structures and transmission coefficient based on the implementation of these measured elastic constants in a finite-element model, and we investigate experimentally and discuss the creation of local resonance band gaps in the studied plates as function of the stub thickness. We confront numerical and experimental results to show the good agreement between both approaches. Finally, conclusions are given in Sec. IV.

### II. MODELS AND EXPERIMENTAL METHODS

Regarding the numerical model, the band structures were computed making use of the finite-element method as

described in our recent work.<sup>6</sup> Because of the periodicity of the structure, which is assumed to be in both  $x$  and  $y$  directions, only one unit cell is considered with periodic boundary conditions for the interfaces between the nearest unit cells according to Bloch-Floquet theorem. The stress-free boundary conditions are used in the other faces, and a fine three-dimensional mesh is chosen. The finite-element method was also used for the calculation of the coefficient transmission. Taking advantage of the periodicity of our LRPCs, a line of 10 stubs was considered on the plate with absorbing boundary conditions (perfectly matched layers) on both sides of the system. The excitation of the out-of-plane waves was done by applying force perpendicular to the plate surface on the side near the first stub, and the displacement field was recorded in the other side near the 10th stub to deduce the transmission coefficient. In our numerical model, the viscoelastic and nonlinear effects of the silicone rubber were not considered, since as we explain later, those effects can be neglected in our structures.

Concerning the experimental approach, the considered 2D phononic plates with a periodic stubbed surface consist of  $10 \times 10$  silicone rubber stubs deposited on a thin aluminum plate 0.5 mm thick. A typical structure is shown in Fig. 1. The period of the structures and the diameter of the stubs are fixed to  $a = 1$  cm and  $d = 6$  mm respectively. Two LR structures were fabricated with different stub thicknesses  $h$  (1.5 and 5 mm). Due to the softness of the used silicone rubber and to ensure the perfect cylindrical shape of stubs, the latter were fabricated using a water jet technique. Perfect rubber stubs were then obtained with the required sizes. Owing to the different types of silicone rubber commercially available, Brillouin spectroscopy<sup>16</sup> was carried out to determine the real

elastic constants of used rubber. In this study, a Methyl Vinyl in polymer (VMQ) silicone rubber was used.<sup>17</sup> The only physical parameters of this type of rubber provided by the producers are the density and the hardness, which equal to  $1300 \text{ kg/m}^3$  and 60 Shore A respectively.

Brillouin spectroscopy is one of the most reliable techniques used to measure the elastic constants of materials. BS is based on the interaction between a photon and an acoustic phonon. The scattered light is composed of elastic and inelastic contributions. The spectrum exhibits the elastic scattered light, also called Rayleigh scattering, and on both sides Stokes and anti-Stokes processes, related to a gain or a loss of energy. The frequency shift between the elastic scattering and the inelastic processes gives direct access to the energy and then to the acoustic wave velocities for transverse, quasitransverse, and longitudinal modes.<sup>18</sup> In our case, the silicone rubber is isotropic, and the elastic constants were determined from the measured phase velocities. For backscattering interaction, the latter are determined directly from the Brillouin spectrum by Eq. (1):<sup>19</sup>

$$V = \lambda_0 \frac{f}{2n} \quad (1)$$

where  $\lambda_0 = 514.4$  nm is the wavelength of the used laser,  $f$  is the frequency of the inelastic diffusion peak (longitudinal and transverse modes), and  $n = 1.45$  is the refraction index of the rubber. Regarding the characterization of acoustical properties of the stubbed plates, a laser ultrasonic experiment has been conducted.<sup>20,21</sup> The considered plates are instrumented with a 5-mm-diameter PZT transducer, placed above the stubbed area (see Fig. 1). The PZT disk is driven by an amplified pseudorandom signal generated by the integrated function generator of a SLDV (Polytec PSV400M2). The plate is held perpendicular with respect to the laser beam through a C-clamp applied to the lower edge, and its response is recorded by the SLDV scanning head placed at a distance of 3 m, which scans the back side of the plate (90 mm square) covered by the rubber array (Fig. 1). No scan of the stubs is performed; only the out-of-plane displacement field of the plate is recorded. The measurement grid is formed by  $N \times N$  points, with  $N = 60$ , and the horizontal and vertical spacing, respectively, are both equal to  $\Delta x_1 = \Delta x_2 = 1.5$  mm. The pseudorandom signal excites the plate in a frequency range from 0.4 to 6 kHz. The sampling frequency of the vibrometer is set equal to 25.6 kHz. The SLDV analysis is carried out in the frequency domain, and thus the output of the laser acquisition is the Fast Fourier Transform (FFT) magnitude of the out-of-plane displacement of every scan point of the grid  $(x_{1j}, x_{2j}, f)$ , where the pair  $(x_{1j}, x_{2j})$  defines the location of the scan point, with  $j = 1, \dots, N^2$ , and  $f$  is the frequency, spanning the excitation range with a resolution  $\Delta f = 3.125$  Hz. The data corresponding to the displacements along the directions of the first irreducible Brillouin zone,  $\hat{u}_r(f)$ , where  $r = 0^\circ, 45^\circ, 90^\circ$  indicates the considered direction (Fig. 1), are extracted from the recorded field  $(x_{1j}, x_{2j}, f)$  according to the following averaging procedure:

$$\hat{u}_r(f) = \frac{1}{N} \sum_{j|(x_{1j}, x_{2j}) \in r} \hat{u}(x_{1j}, x_{2j}, f). \quad (2)$$

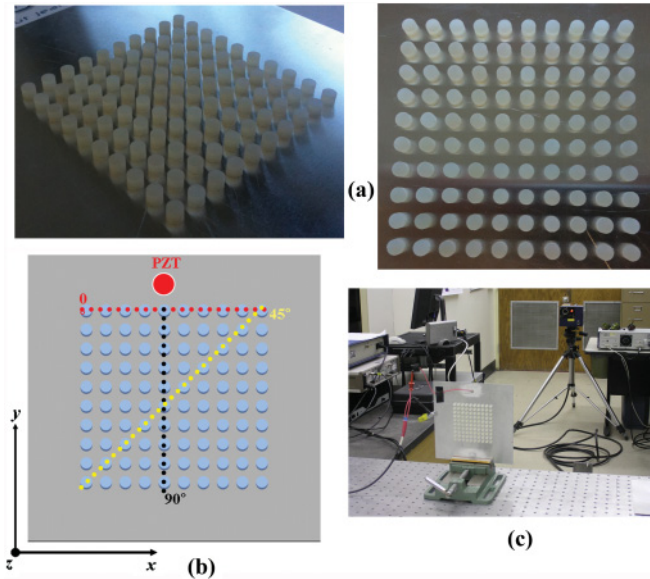


FIG. 1. (Color online) (a), (b) Phononic plates with a periodic stubbed surface consisting of  $10 \times 10$  silicone rubber stubs deposited on a thin aluminum plate 0.5 mm thick. The red circle represents an example of the location of the PZT transducer for elastic wave excitation and the dotted lines represent the line scans along  $0^\circ$ ,  $45^\circ$ , and  $90^\circ$ . (c) The measurement setup showing the plate with the PZT transducer and the laser beam in the background.

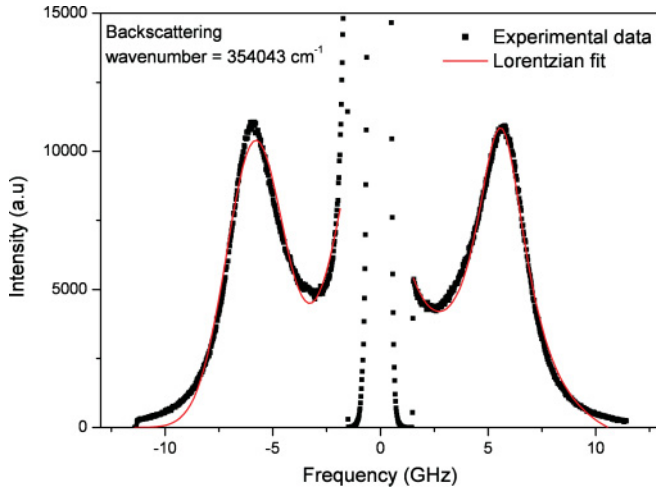


FIG. 2. (Color online) Brillouin spectrum of the silicone rubber (1.5 mm thick) showing symmetrical longitudinal mode peaks at 5.5 GHz.

### III. EXPERIMENTAL MEASUREMENTS

#### A. Characterization of acoustic properties of silicone rubber

As mentioned in the previous paragraph, many types of silicone rubber exist. We used Brillouin spectroscopy to measure the elastic constants of the used rubber. This measurement is not straightforward since the concerned material is very soft and lossy. Consequently, the velocity and coupling of shear modes should be very low. BS analysis was performed on a piece of silicone rubber. Figure 2 shows a typical obtained Brillouin spectrum. First, besides the elastic diffusion (central peak), one can observe only strong symmetric peaks at  $f = 5.5$  GHz, which correspond to longitudinal modes. Based on Eq. (1), the measured longitudinal velocity of silicone rubber is about of  $V_l = 975$  m/s. Taking into account the density value, the longitudinal elastic constant is equal to  $c_{11} = 1.23$  GPa. Regarding the shear velocity  $V_t$ , the latter is too small and hardly measurable by Brillouin spectroscopy (very weak optical anisotropy), and therefore it is more reliable to estimate it by a different approach. The value of shear velocity has actually a great importance in the determination of the LR BG localization. Primary numerical simulations were performed (not shown here) and indicate a significant influence of the shear velocity value on the localization of the BG. Based on those primary computations and on an estimation using the hardness value of the used silicone rubber ( $H = 60$  Shore A), a shear velocity of  $V_t = 23.53$  m/s was determined. Table I summarizes the physical properties we used for the silicone rubber and aluminum.

TABLE I. Physical properties of the used silicone rubber and aluminum.

	$\rho$ (kg/m <sup>3</sup> )	$c_{11}$ (GPa)	$c_{44}$ (MPa)	$c_{12}$ (MPa)	$V_l$ (m/s)	$V_t$ (m/s)	$E$ (GPa)	$\nu$
Silicon rubber	1300	1.23	0.7199	$c_{11} - 2c_{44}$	975	23.53	2.15	0.4998
Aluminium	2702	107.3	$2.83 \times 10^4$	$6.08 \times 10^4$	6301.7	3236.3	70	0.33

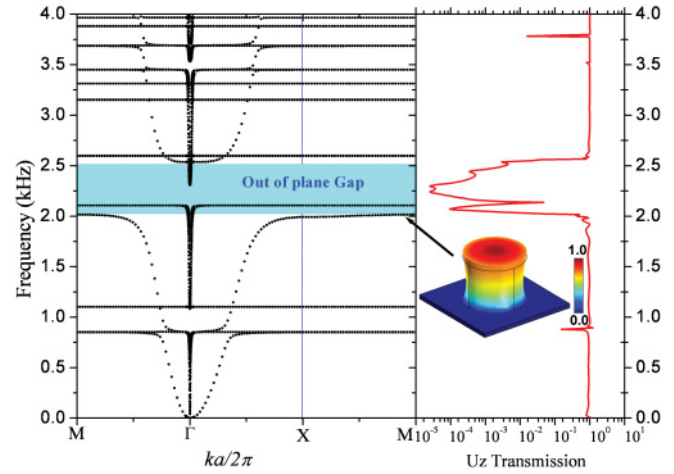


FIG. 3. (Color online) Computed band structure and out-of-plane modes' transmission coefficient of the LRPC plate having stubs 5 mm high, showing an out-of-plane BG (gray; cyan online). The inset exhibits the displacement field of the elongation mode responsible for the out-of-plane BG, corresponding to the wave vector indicated by the arrow.

#### B. Experimental evidence of LR sonic band gap

The elastic properties of silicone rubber (determined above) and aluminum were introduced as inputs to our finite-element model,<sup>22</sup> which computes the band structure and the transmission coefficient of the different fabricated structures. Here, we present the results concerning the stubs 5 and 1.5 mm high.

We consider first the sample with 5-mm stubs. The calculated band structure and transmission of the LRPC of this sample is depicted in Fig. 3. Since we access only the out-of-plane modes by SLDV measurements, we focus here only on the out-of-plane mode band gap. This gap is shown in cyan in Fig. 3 and extends from 2.02 to 2.53 kHz, while the complete LR BG (all polarizations) is narrower and extends from 2.1 to 2.3 kHz. The finite-element method allows the calculation of modal displacements, by which we can determine the polarization of each branch in the band structure and then recognize the nature of the BG. The stub eigenmode responsible for the out-of-plane BG is the elongation mode (inset in Fig. 3), which has mainly an out-of-plane polarization so that it couples with the out-of-plane modes of plate and opens the BG.<sup>6</sup> The calculated transmission of the out-of-plane mode ( $U_z$  polarization) matches very well with the band structure and then corroborates the obtained gap. Experimental characterization making use of SLDV was performed along different directions of the first Brillouin zone, as shown in Fig. 4. Displacement fields of the out-of-plane modes were analyzed in a frequency range extending from 0.4 to 6 kHz. The recorded displacement field  $\hat{u}_r(f)$  is plotted for all considered directions. An evident attenuation of the wave field around

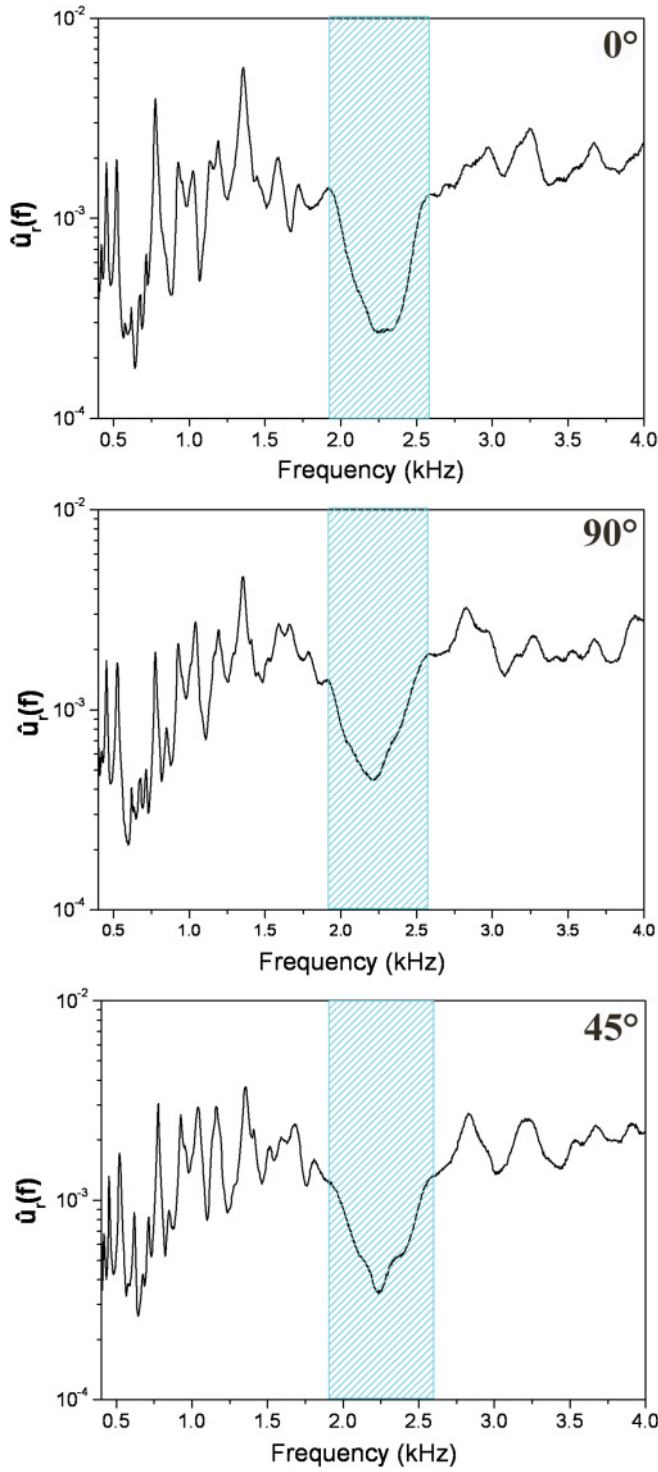


FIG. 4. (Color online) SLDV measurements of LRPC plate having stubs 5-mm high and 6 mm in diameter along directions  $0^\circ$ ,  $45^\circ$ , and  $90^\circ$ , which correspond to horizontal, diagonal, and vertical ones. The curves represent the recorded displacement field  $\hat{u}_r(f)$  as function of the frequency, showing a significant attenuation of the wave field and implying a presence of a BG.

$f = 2.25$  kHz is observed, implying the presence of a BG. Indeed, in this figure, the recorded field along the different direction of first Brillouin zone shows a strong attenuation from 1.925 to 2.58 kHz. This measured band gap agrees very

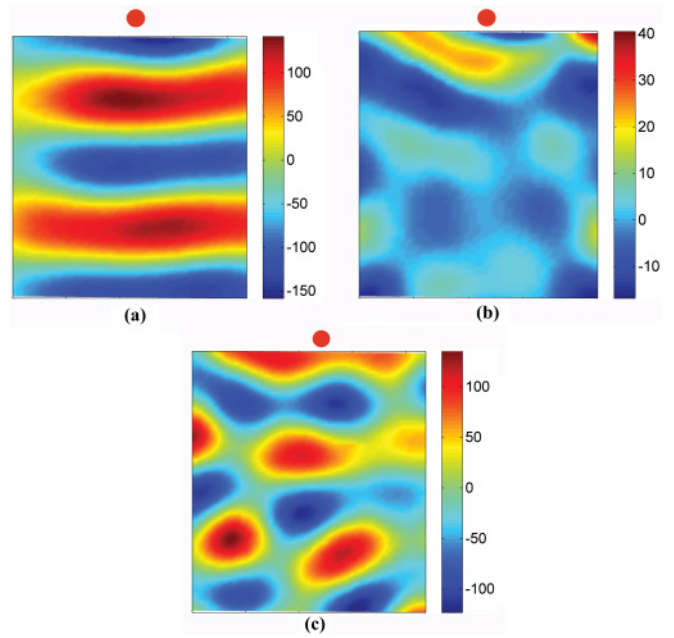


FIG. 5. (Color online) Experimental measurements obtained by SLDV showing three steady-state deformed shapes, representing the stationary response of the plate (5 mm stub height) corresponding to an excitation below the BG at 1.359 kHz (a), inside the BG at 2.234 kHz (b), and above the BG at 2.828 kHz (c). The red circle represents the excitation source of the elastic waves.

well with the computed one, which extends from 2.02 to 2.53 kHz. Regarding the shallow nature of the attenuation, since the LR BG is large enough in that case owing to the wide resonant band of the single unit (low quality factor), the penetration depth of the wave is large, then a shallow attenuation peak is recorded.

To illustrate the behavior of the LRPC plate in the studied frequency range, Fig. 5 shows three steady-state deformed shapes of the structure, corresponding to an excitation below the BG [Fig. 5(a)], inside the BG [Fig. 5(b)], and above the

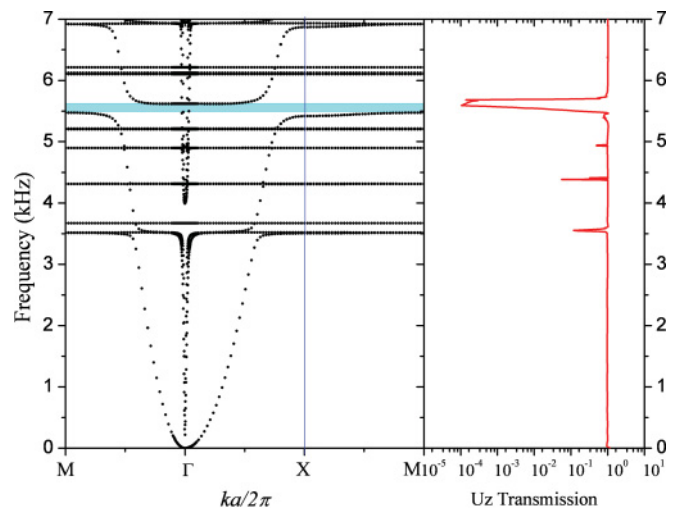


FIG. 6. (Color online) Computed band structure and out-of-plane mode transmission coefficient of the LRPC plate having stubs 1.5 mm high, showing a very narrow out-of-plane BG (gray; cyan online).

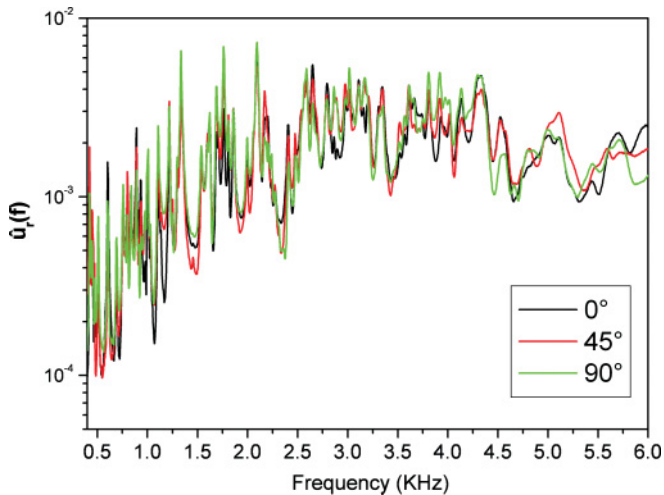


FIG. 7. (Color online) SLDV measurements of LRPC plate having 1.5-mm-high stubs along directions  $0^\circ$ ,  $45^\circ$ , and  $90^\circ$ , which correspond to horizontal, diagonal, and vertical ones. The curves represent the recorded displacement field  $\hat{u}_r(f)$  as function of the frequency. No evident attenuation is observed.

BG [Fig. 5(c)]. These are not snapshots of the wave field, but stationary plate responses for a given frequency of excitation. These figures are obtained from the SLDV, extracting the displacement field from the data acquisition for a selected frequency. It is interesting to observe that, for the BG case, the plate is almost undeformed, because the energy is reflected by the rubber resonators, and the energy provided by the excitation remains confined near the source (located at the middle of the right vertical boundary of the measured region; see Fig. 5). However, in the first and in the third cases, the plates undergo deformation according their modal shapes.

Similar investigations are conducted on the second structure, the plate with 1.5-mm-high stubs. The computed band structure and transmission are given in Fig. 6. These numerical results show a very narrow out-of-plane mode BG localized from 5.49 to 5.62 kHz, while no complete BG is obtained. In addition, the out-of-plane transmission mode shows the same obtained BG. The measured displacement fields through the structure and along the different directions of the first Brillouin zone are illustrated in Fig. 7. One can observe that no clear BG is obtained in the studied frequency range, extended from 0.4 to 6 kHz, although a different behavior of the wave-field signal between 5.25 to 5.8 kHz can be seen. The non-observation of a clear BG for this 1.5-mm-stub structure can be explained by its narrow nature, as observed in the calculated results. The second reason may be the rough quality of excitation above 4 kHz, which can complicate the visualization of the BG. In spite of this, we can conclude that moderate agreement between numerical and experimental results for

the 1.5-mm-stub structure is obtained. The dependence of the BG localization on the stub height can be easily explained by a spring mass model. Recently, we reported on a detailed theoretical study of stubbed LR plates and we discussed in detail the physics behind the creation and the localization of this BG as function of the geometrical parameters of the structure.<sup>6</sup> Indeed, decreasing the stub height (from 5 to 1.5 mm) increases its resonance frequencies, implying the moving of BG localization to higher frequencies.

Regarding the viscoelastic effect and its contribution in the spectral attenuation, we make different observations that allow us to conclude that this effect is negligible in our structures. First, if the viscoelastic losses are dominant, significant attenuation should be recorded for the 1.5-mm LRPC structure too, which is not the case. Second, we used a medium silicone rubber which is less lossy than the usual soft ones. Third, we are in the low-frequency regime in which the viscoelastic effect is much lower than in the high-frequency one, since it increases linearly with the frequency. Then, we can conclude that the recorded attenuations are due to the local resonance mechanism. On the other hand, concerning the nonlinear effect, basically, it can be neglected even for the strong nonlinear materials when the amplitude of the wave is small, which is the case in our structures.

Based on the experimental and numerical results we presented here, a sonic BG around 2.2 kHz was obtained with a locally resonant phononic plate having a 1-cm lattice period. The wavelengths in such a structure, taking into account the material composition of the plate, are much larger than the period. To appreciate this difference in terms of frequency, the Bragg BG allowed in our structure should be located approximately at 152 kHz. Thus, based on the obtained results, we show that a LRPC system for low-frequency shielding applications with much reduced sizes can be concretely considered and performed.

#### IV. CONCLUSIONS

We experimentally investigated a two-dimensional locally resonant phononic crystal composed of periodic arrangement of silicone rubber stubs deposited on a thin aluminum plate. We analyzed the physical properties of the used silicone rubber as it plays a key role in the structure behavior and input those parameters into an efficient finite-element method to approach theoretically the behavior of the plates. We showed that the structure proposed here can be fabricated easily and the physics behind it can be presented clearly. A locally resonant sonic BG around 2.2 kHz was experimentally observed, and good agreement between theoretical and experimental approaches was obtained. The results suggest the possibility of building simple LR systems with reduced sizes for low-frequency applications.

\*badreddine.assouar@gatech.edu

<sup>1</sup>M. Sigalas and E. N. Economou, *Solid State Commun.* **86**, 141 (1993).

<sup>2</sup>M. S. Kushwaha, P. Halevi, L. Dobrzynski, and B. Djafari-Rouhani, *Phys. Rev. Lett.* **71**, 2022 (1993).

<sup>3</sup>C. Huang, J.-H. Sun, and T.-T. Wu, *Appl. Phys. Lett.* **97**, 031913 (2010).

<sup>4</sup>Z. Liu, X. Zhang, Y. Mao, Y. Y. Zhu, Z. Yang, C. T. Chan, and P. Sheng, *Science* **289**, 1734 (2000).

- <sup>5</sup>T. Still, G. Gantzounis, D. Kiefer, G. Hellmann, R. Sainidou, G. Fytas, and N. Stefanou, *Phys. Rev. Lett.* **106**, 175505 (2011).
- <sup>6</sup>M. Oudich, Y. Li, M. B. Assouar, and Z. Hou, *New. J. Phys.* **12**, 083049 (2010).
- <sup>7</sup>C. Goffaux, J. Sanchez-Dehesa, A. Levy Yeyati, P. Lambin, A. Khelif, J. O. Vasseur, and B. Djafari-Rouhani, *Phys. Rev. Lett.* **88**, 225502 (2002).
- <sup>8</sup>H. Larabi, Y. Pennec, B. Djafari-Rouhani, and J. O. Vasseur, *Phys. Rev. E* **75**, 066601 (2007).
- <sup>9</sup>Y. Pennec, B. Djafari-Rouhani, H. Larabi, J. O. Vasseur, and A. C. Hladky-Hennion, *Phys. Rev. B* **78**, 104105 (2008).
- <sup>10</sup>T.-T. Wu, Z. G. Huang, T.-C. Tsai, and T.-C. Wu, *Appl. Phys. Lett.* **93**, 111902 (2008).
- <sup>11</sup>J. S. Hsu and T.-T. Wu, *Appl. Phys. Lett.* **90**, 201904 (2007).
- <sup>12</sup>G. Wang, X. S. Wen, J. H. Wen, L. H. Shao, and Y. Z. Liu, *Phys. Rev. Lett.* **93**, 154302 (2004).
- <sup>13</sup>Z. Y. Cui, T. N. Chen, H. L. Chen, and Y. P. Su, *Appl. Acoust.* **70**, 1087 (2009).
- <sup>14</sup>M. Hirsekorn, P. P. Delsanto, A. C. Leung, and P. Matic, *J. Appl. Phys.* **99**, 124912 (2006).
- <sup>15</sup>W. Xiao, G. W. Zeng, and Y. S. Cheng, *Appl. Acoust.* **69**, 255 (2008).
- <sup>16</sup>J. Kruger and H. G. Unruh, *Solid State Commun.* **21**, 583 (1977).
- <sup>17</sup>[[www.trelleborg.com/industrialhose](http://www.trelleborg.com/industrialhose)].
- <sup>18</sup>W. Hayes and R. Loudon, *Scattering of Light by Crystals* (Dover, New York, 1978).
- <sup>19</sup>J. Eschbach, B. Vincent, D. Rouxel, M. El Hakiki, and O. Elmazria, *IEEE Trans. Ultrason. Ferroelectr. Freq. Control* **56**, 644 (2009).
- <sup>20</sup>W. J. Staszewski, B. C. Lee, L. Mallet, and F. Scarpa, *Smart Mater. Struct.* **13**, 251 (2004).
- <sup>21</sup>J. E. Michaels, T. E. Michaels, and M. Ruzzene, *Ultrasonics* **51**, 452 (2011).
- <sup>22</sup>M. Oudich, M. B. Assouar, and Z. Hou, *Appl. Phys. Lett.* **97**, 193503 (2010).